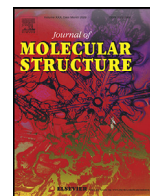




Since January 2020 Elsevier has created a COVID-19 resource centre with free information in English and Mandarin on the novel coronavirus COVID-19. The COVID-19 resource centre is hosted on Elsevier Connect, the company's public news and information website.

Elsevier hereby grants permission to make all its COVID-19-related research that is available on the COVID-19 resource centre - including this research content - immediately available in PubMed Central and other publicly funded repositories, such as the WHO COVID database with rights for unrestricted research re-use and analyses in any form or by any means with acknowledgement of the original source. These permissions are granted for free by Elsevier for as long as the COVID-19 resource centre remains active.



Large interfacial relocation in RBD-ACE2 complex may explain fast-spreading property of Omicron

Maryam Shirzadeh, Hassan Monhemi*, Mohammad Eftekhari

Departament of Chemistry, Faculty of Science, University of Neyshabur



ARTICLE INFO

Article history:

Received 17 March 2022

Revised 7 July 2022

Accepted 31 July 2022

Available online 31 July 2022

Keywords:

SARS-CoV-2

Variant

Omicron

Binding interface

ABSTRACT

The Omicron variant of SARS-CoV-2 emerged in South African in late 2021. This variant has a large number of mutations, and regarded as fastest-spreading Covid variant. The spike RBD region of SARS-CoV-2 and its interaction with human ACE2 play fundamental role in viral infection and transmission. To explore the reason of fast-spreading properties of Omicron variant, we have modeled the interactions of Omicron RBD and human ACE2 using docking and molecular dynamics simulations. Results show that RBD-ACE2 binding site may drastically relocate with an enlarged interface. The predicted interface has large negative binding energies and shows stable conformation in molecular dynamics simulations. It was found that the interfacial area in Omicron RBD-ACE2 complex is increased up to 40% in comparison to wild-type Sars-Cov-2. Moreover, the number of hydrogen bonds significantly increased up to 80%. The key interacting residues become also very different in Omicron variant. The new binding interface can significantly accommodate R403, as a key RBD residue, near ACE2 surface which leads to two new strong salt bridges. The exploration of the new binding interface can help to understand the reasons of high transmission rate of Omicron.

© 2022 Elsevier B.V. All rights reserved.

1. Introduction

Coronavirus disease 2019 (COVID-19) induced by the invasion of severe acute respiratory syndrome coronavirus 2 (SARS-CoV-2) has been quickly spreading all over the world since December 2019 [1,2]. It has led to more than 275 million infected patients and over five million deaths up to December 2021 [3]. SARS-CoV-2 infection is mainly mediated by the molecular interactions between the spike protein (S-pro) of the virus and the host angiotensin-converting enzyme II (ACE2) in human [4,5]. While currently there is no proven effective medications or therapy options for the treatment of this contagious disease, there are serious concerns about the new variants with higher spreading rates and stronger infection abilities [6]. Vaccines represent the most efficient means to control and stop the pandemic of COVID-19 [7]. It was shown that the designated vaccines have reassuring safety and could effectively reduce the death, severe cases, symptomatic cases, and infections resulting from SARS-CoV-2 through the world [8]. However, the new SARS-CoV-2 variants reduces the hopes to the vaccines [9–11]. WHO has characterized some specific variants as Variants of Interest (VOIs) and Variants of Concern (VOCs), in order to prioritize global monitoring and research, and ultimately to

inform the ongoing response to the COVID-19 pandemic. The Technical Advisory Group on SARS-CoV-2 Virus Evolution (TAG-VE) was convened on 26 November 2021 to assess the SARS-CoV-2 variant: B.1.1.529 as a new VOC and named it as “Omicron”. Omicron variant was first reported to WHO from South Africa on 24 November 2021. Omicron is a species with the most diverse mutations detected during an epidemic, raising serious concerns that it may be associated with a significant reduction in vaccine efficacy and an increased risk of re-infection. Several changes in the spike protein-encoding sequence are associated with increased transmissibility, immune escape, or other properties. In total, more than 60 substitutions/deletions/insertions have been verified in the Omicron variant [12]. This is the largest number of mutation sites of all SARS-CoV-2 variants characterized to this time. More than half of the total Omicron identified mutations are appeared in the spike [12]. These mutations include 30 substitutions (A67V, T95I, Y145D, L212I, G339D, S371L, S373P, S375F, K417N, N440K, G446S, S477N, T478K, E484A, Q493R, G496S, Q498R, N501Y, Y505H, T547K, D614G, H655Y, N679K, P681H, N764K, D796Y, N856K, Q954H, N969K, and L981F), three deletions (H69/V70, G142/V143/Y144 and N211), and one insertion (three amino acids (EPE) at position 214). Out of these, 15 mutations occur in receptor binding motif of RBD (G339D, S371L, S373P, S375F, K417N, N440K, G446S, S477N, T478K, E484A, Q493R, G496S, Q498R, N501Y, Y505H). The locations of these mutations are depicted in Fig. 1. The rapid replacement of the delta type by Omicron

* Corresponding author.

E-mail address: h.n.monhemi@gmail.com (H. Monhemi).

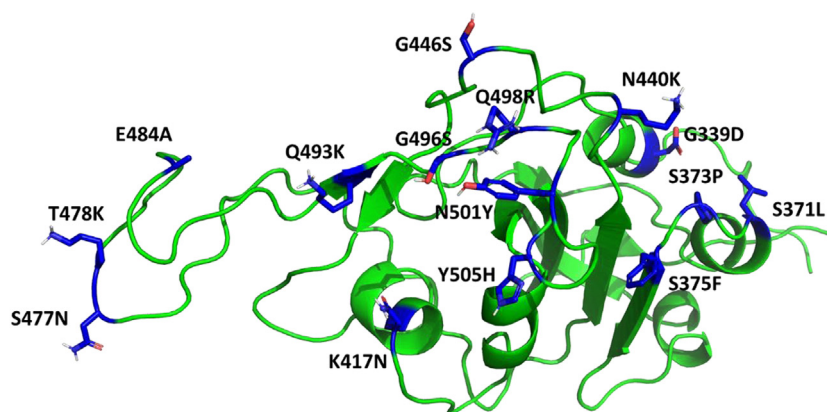


Fig. 1. The locations of mutations in receptor binding motif of Omicron RBD

in South Africa raises concerns that this type of delta is more contagious, although the number of COVID-19 cases in South Africa is currently small, which could have a proportionate effect on both. In order to obtain new structural insights about the fast-spreading properties of Omicron, we have explored the molecular interactions between Omicron RBD and ACE2 using Docking and Molecular Dynamics (MD) simulations. The results showed that Omicron spike may bind to ACE2 with distinct binding site with diverse interaction residues.

2. Methods

The crystal structure of wild-type Sars-Cov-2 (PDB:6m0j [13]) was obtained from protein data bank and used as template for the calculations. The structures of RBD and ACE2 were separated as single PDB files for subsequent calculations. SWISS-MODEL [14] was used to construct RBD of Omicron and to locate the mutations in wild-type template. Protein-protein docking calculations were performed by HADDOCK as one of the most reliable docking tools for protein-protein complexes [15,16]. The active residues were selected based on the interacting residues of wild-type RBD-ACE2 complex [13] (ACE2: 24, 30, 31, 35, 37, 38, 41, 42 RBD: 417, 446, 449, 487, 489, 493, 500, 501, 502, and 505). To include the role of new mutations of Omicron in RBD-ACE2 interface, the mutations in the interface were considered as active residues in docking calculations (Fig. 1). HADDOCK clustered 167 structures in 8 clusters, which represents 83.5% of the water-refined models HADDOCK generated. Top clusters based on the energies of binding are demonstrated in Table 3. The best score is obtained for Cluster 3 with very high HADDOCK score (-187.2 +/- 5.1). As the differences in energies was significantly high between Cluster 3 and other clusters, this cluster was selected for subsequent calculations.

The high-ranked complex obtained from docking calculations were used for MD simulations. All MD simulations were performed by GROMACS 2019 package. The parameters of SPC/E model was used for water molecules [17]. GROMOS96 (GROMOS 43a1) force field was used for proteins [18]. In the first stage of simulation, periodic simulation boxes were constructed and one RBD-ACE2 complex was putted in each box. The box size was chosen so that the minimal distance of complex atoms from the wall was greater than 1 nm. Then, each system was solvated by water molecules. The Berendsen algorithm [19] was used to control pressure and temperature during simulations. The temperature and pressure were set to 298 K and 1 bar. After energy minimization of the boxes, each system was equilibrated for 100 ps in an NVT ensemble at specified temperature. A 100 ps MD simulation was carried out in the NPT ensemble at the same temperature and at constant pressure. Then, 200 ns equilibration simulation was performed for each

system. To neutralize the systems, sodium and chloride ions were added to the simulation boxes. Each simulation was repeated three times with the different initial conditions to increase the precision of the simulations and to prevent any dependencies of the results on the initial conditions. Energy minimization was performed using steepest-descent algorithm. SETTLE and LINCS algorithms were used to fix chemical bonds during the simulations [20,21]. Electrostatic interactions were estimated by Particle Mesh Ewald (PME) algorithm [22]. Graphical representations were created by PyMOL software [23]. Interfacial analysis were performed by COCOMAPS [24].

3. Results and discussion

3.1. New binding site assignment for Omicron spike

The overall structures of the RBD-ACE2 binding interface were relatively similar in SARS-CoV and SARS-CoV-2 [13,25]. Receptor binding motif (RBM) of RBD forms a gently concave surface with a ridge on one side; it binds to the exposed outer surface of the claw-like structure of ACE2 in both strains [13,25]. VOCs such as Kappa and Delta also showed similar binding interfaces on ACE2 [26]. We have docked RBD to ACE2 for Omicron and wild type of SARS-CoV-2 using HADDOCK as one of the most reliable docking tools for protein complexes [15,16]. The structure of the top-ranked RBD-ACE2 cluster is selected based on the minimum energy of docking (see method section). Structural alignment of the predicted complexes for wild-type Sars-Cov-2 and Omicron variant along with the crystal structure of RBD-ACE2 complex are shown in Fig. 2.

As shown in this figure, the binding interface of Omicron RBD substantially deviates from wild SARS-CoV-2 and shows a structural relocation. The predicted binding site of the docked complex of the wild-type is very similar to the aligned crystal structure (PDB:6m0j[13]), showing the reliability of docking algorithm. Moreover, all of the experimentally reported interactions were reproduced correctly (see section 2.3). To have more clear representation, the interaction of RBD-ACE2 is shown by surface representation in Fig. 3.

The relocation and enlargement of the interface are clearly represented in this figure. Moreover, the interface area of RBD-ACE2 complex is substantially increased (about 40%) from wild-type Sars-Cov and Sars-Cov-2 to Omicron variant (Fig. 3 (c)). Both polar and non-polar interface are increased in Omicron complex. Moreover, it can be seen that in all strains the polar interface area is higher than non-polar interface area. This shows that RBD interacts with ACE2 mostly through the polar interactions, which is consistent with the experimental observations [13,25].

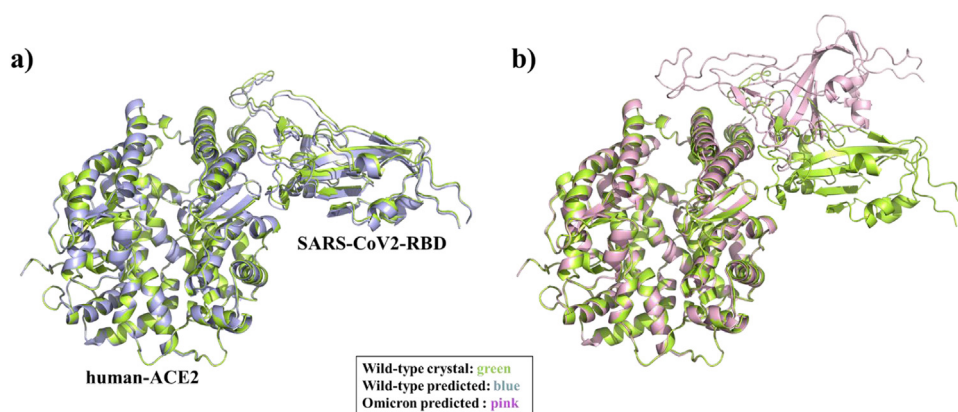


Fig. 2. Structural alignment of RBD-ACE2 complexes in the different forms

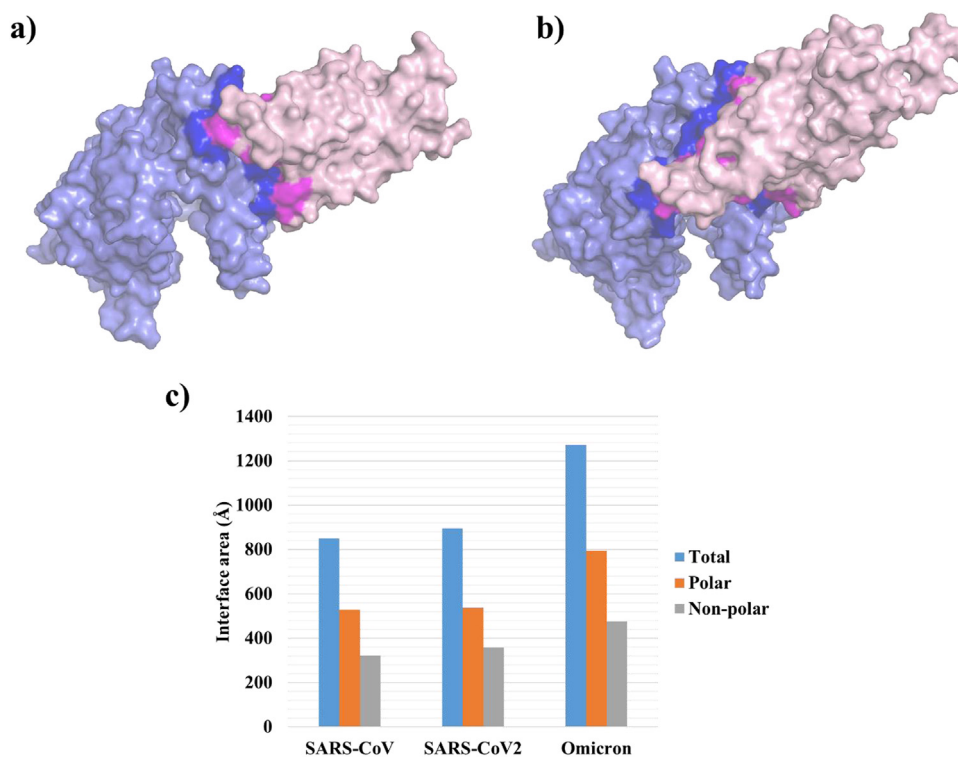


Fig. 3. Surface representation of (a) wild-type Sars-Cov-2 RBD-ACE2 complex, (b) Omicron RBD-ACE2 complex, and (c) interface area of RBD-ACE2 complexes in the different strains

3.2. MD simulation of ACE2-RBD complexes

Application of MD simulations to optimize and validate of the docking complexes is a common practice in molecular biology and drug discovery [27–29]. If the obtained protein-protein complexes show reasonable stability and dynamics in MD simulations, the atomic level interactions between two proteins become interpretable. To validate the obtained complex for Omicron variant, MD simulations of the predicted wild-type and Omicron RBD-ACE2 complex were performed. Root mean square deviation (rmsd) is a parameter which shows the stability and association/dissociation behavior of protein-protein complexes [30]. Higher rmsd values show the lower stability and dissociation behavior of the complexes. Rmsd values of the Sars-Cov-2 and Omicron RBD-ACE2 complexes, which is obtained by comparison of C-alpha carbon atoms, are shown in Fig. 4. As shown in this figure, after initial reasonable increases (to about 0.25nm), rmsd of both RBD-ACE2 complexes reach to constant equilibrium values. The values are in

similar ranges which indicates that the complex is stable in both wild-type and Omicron variant.

Root mean square fluctuation (rmsf) is a dynamical analysis in MD simulations and shows the mobility and flexibility of residues in protein complexes [31]. Higher rmsf values show the higher mobility and lability of interacting residues. Rmsf values for the residues of wild-type and Omicron RBD-ACE2 complexes are shown in Fig. 5. As shown in the figure, the interacting residues of both the complexes show low and comparable fluctuations. This also confirms the stability and robustness of the binding site interactions for the predicted RBD-ACE2 complexes.

3.3. Structural analysis of the new interface for Omicron

Our docking and simulation results confirm a new binding mechanism for Omicron which was never seen before for SARS-CoV-2 and its variants. The interacting residues at the interfaces of wild-type and Omicron RBD-ACE2 complex are highlighted in

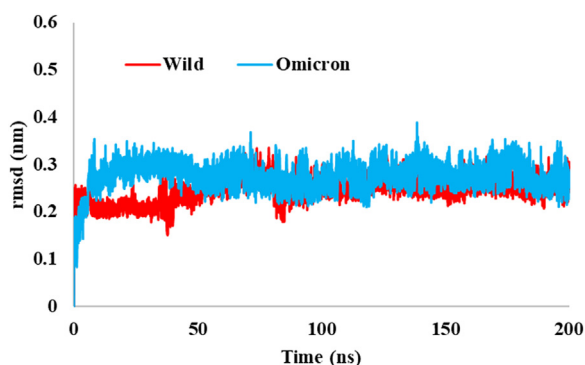


Fig. 4. Rmsd values of RBD-ACE2 complexes

Fig. 6. As shown in this figure, the shape of the interface and also binding residues become drastically different in Omicron variant in comparison to wild-type Sars-Cov-2. One of the most important features of RBD-ACE2 interfaces in both Sars-Cov and Sars-Cov-2 variants is the networks of hydrophilic interactions and hydrogen bonds [13,32]. The number of interfacial hydrogen bonds are 13 in both Sars-Cov and Sars-Cov-2 RBD-ACE2 complexes [13].

An energetically significant hydrogen bond occurs when donor and acceptor atoms are within about 3.5 Å. With this cut-off distance the number of hydrogen bond with significant electrostatic energies is 11 for Sars-Cov-2 RBD-ACE2 complex. The interfacial residues with hydrogen bond interactions in wild-type and Omicron complexes (cut-off= 3.5 Å) are depicted in Table 1. Interestingly, the number of hydrogen bonds are significantly increased from wild-type Sars-Cov-2 (11) to Omicron variant (20). This shows

Table 1

The hydrogen bonds at the SARS-CoV-2 RBD-ACE2 and Omicron RBD-ACE2 interfaces

Sars-CoV-2 RBD	Length (Å)	ACE2	Length (Å)	Omicron RBD
		Ser19(OG)	2.93	Gln414(NE2)
		Ser19(N)	3.24	Gln414(NE1)
Asn487(ND2)	2.6	Gln24(OE1)		
Lys417(NZ)	3.0	Asp30(OD2)	2.68	Arg408(NH2)
		Asp30(OD2)	3.07	Arg408(NH1)
		Lys31(NZ)	2.6	Glu406(OE2)
		Lys31(NZ)	2.73	Asn417(OD1)
		Lys31(NZ)	2.79	Tyr495(OH)
		His34(O)	3.04	Tyr501(OH)
Gln493(NE2)	2.8	Glu35(OE2)	3.24	Tyr453(OH)
		Glu35(OE1)	2.64	Arg403(NH1)
		Glu35(OE1)	2.79	Ser496(N)
		Glu35(OE1)	2.80	Ser496(OG)
		Glu35(OE1)	3.07	Arg403(NH2)
Tyr505(OH)	3.2	Glu37(OE2)		
		Asp38(OD2)	3.21	Arg498(HE)
Tyr449(OH)	2.7	Asp38(OD2)	2.64	Tyr449(OH)
Thr500(OG1)	2.6	Tyr41(OH)		
Gly446(O)	3.3	Gln42(NE2)		
Tyr449(OH)	3.0	Gln42(NE2)	2.72	Ty449(OH)
		Glu75(OE2)	2.65	Lys493(NZ)
		Glu75(OE2)	2.65	Lys493(NZ)
Tyr489(OH)	3.5	Tyr83(OH)		
Asn487(OD1)	2.7	Tyr83(OH)		
		Ser106(O)	3.37	Asn487(ND2)
		Glu110(OE2)	2.55	Lys478(NZ)
Gly502(N)	2.8	Lys353(O)		

about 80% increase in hydrogen bond ability of Omicron in comparison to wild-type Sars-Cov-2. Based on the distances of hydrogen bonds, most of the interactions in Omicron are strong hydrogen bonds. Moreover, the locations of hydrogen bonds are signifi-

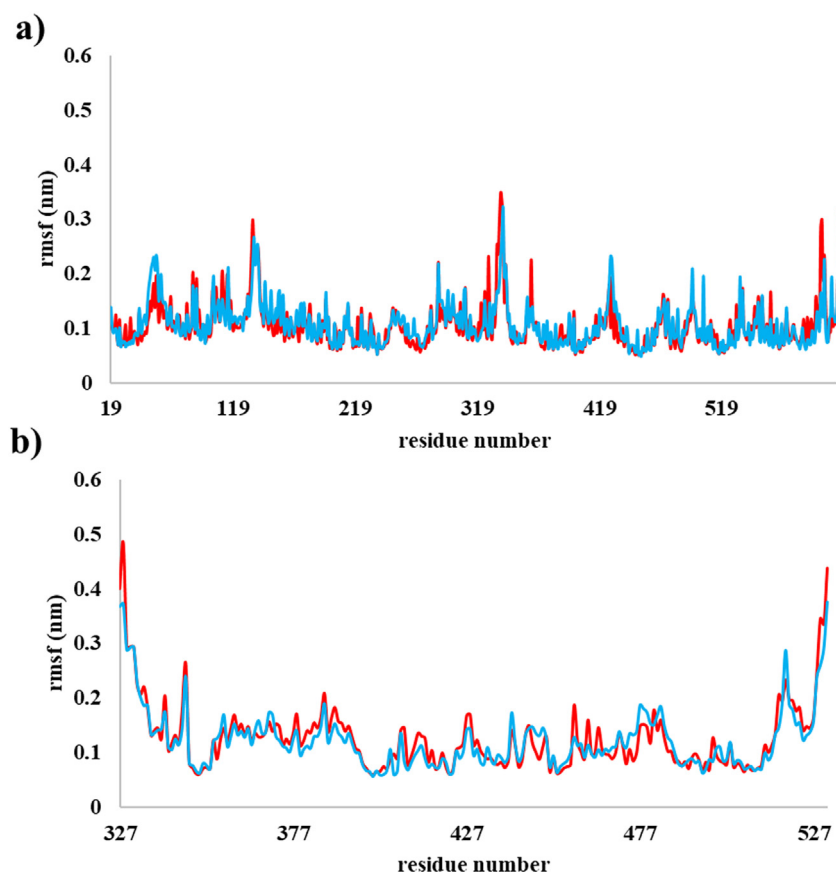


Fig. 5. Rmsf values of (a) ACE2 and (b) RBD in RBD-ACE2 complexes (colors are based on Fig. 4)

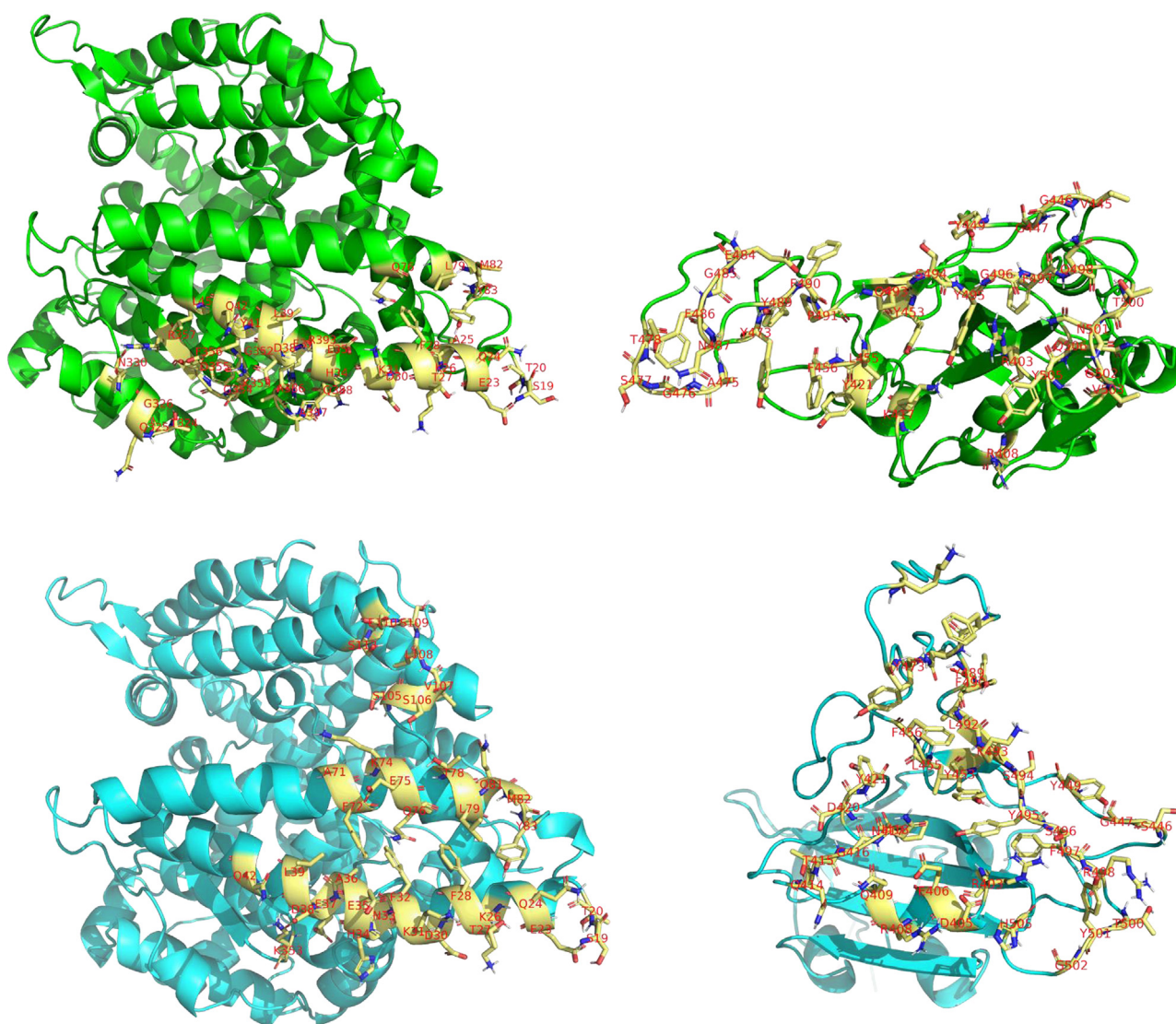


Fig. 6. Interfaces of ACE2 (left) in complex with RBD (right) in wild-type (top) and Omicron (bottom)

cantly different in wild-type Sars-Cov-2 and Omicron. These results may explore the reasons of fast-spreading of Omicron.

In protein-protein interactions a small set of residues contributes the most to binding, the so-called binding Hot-Spots (HS) [33]. A generally accepted definition for HS residues are those site where alanine mutation generate a significant binding free energy difference ($\Delta\Delta G_{\text{binding}} \geq 2.0 \text{ kcal/mol}$ [34]. Here, we estimated HS for the produced complexes using SpotOn [35]. We assigned the key interfacial interactions based on HS and their interacting residues. Table 2 shows key interactions of wild-type Sars-Cov-2 and Omicron RBD-ACE2 complexes. The key interactions are significantly different in two complexes. The only common interaction is hydrogen bond of Ser38 of ACE2 to Tyr449 of RBD. Interestingly, about 50% of key interacting residues of RBD in Omicron variant are the mutated residues (highlighted with red color). This shows how the multiple mutations of RBD in Omicron helps to better binding to ACE2.

The key interaction sites on ACE2 are Gln24, Asp38, Tyr41, Tyr83, and Lys353 for wild-type and Lys31, Glu35, Asp38, and Glu75 for Omicron. We found that Omicron RBD make very different interactions at ACE2 surface. These interactions are graphically represented in Fig. 7. Lys31 and Glu35 of ACE2 make pivotal roles in binding of Omicron RBD. These two residues make many

Table 2

Key interacting residues of SARS-CoV-2 RBD-ACE2 and Omicron RBD-ACE2 interfaces

Sars-CoV-2 RBD	ACE2	Omicron RBD
Asn487	Gln24	Glu406
	Lys31	Asn417
	Lys31	Tyr495
	Glu35	Tyr453
	Glu35	Arg403
	Glu35	Ser496
	Glu35	Ser496
	Glu35	Arg403
	Asp38	Arg498
Tyr449	Asp38	Tyr449
Thr500	Tyr41	
	Glu75	Lys493
	Glu75	Lys493
Asn487	Tyr83	
Gly502	Lys353	

hydrogen bonds with RBD in Omicron (8 hydrogen bonds) while there is only one hydrogen bond for Glu35 in wild-type Sars-Cov-2 (Tables 1 and 2, Fig. 7(a) and 7(d)).

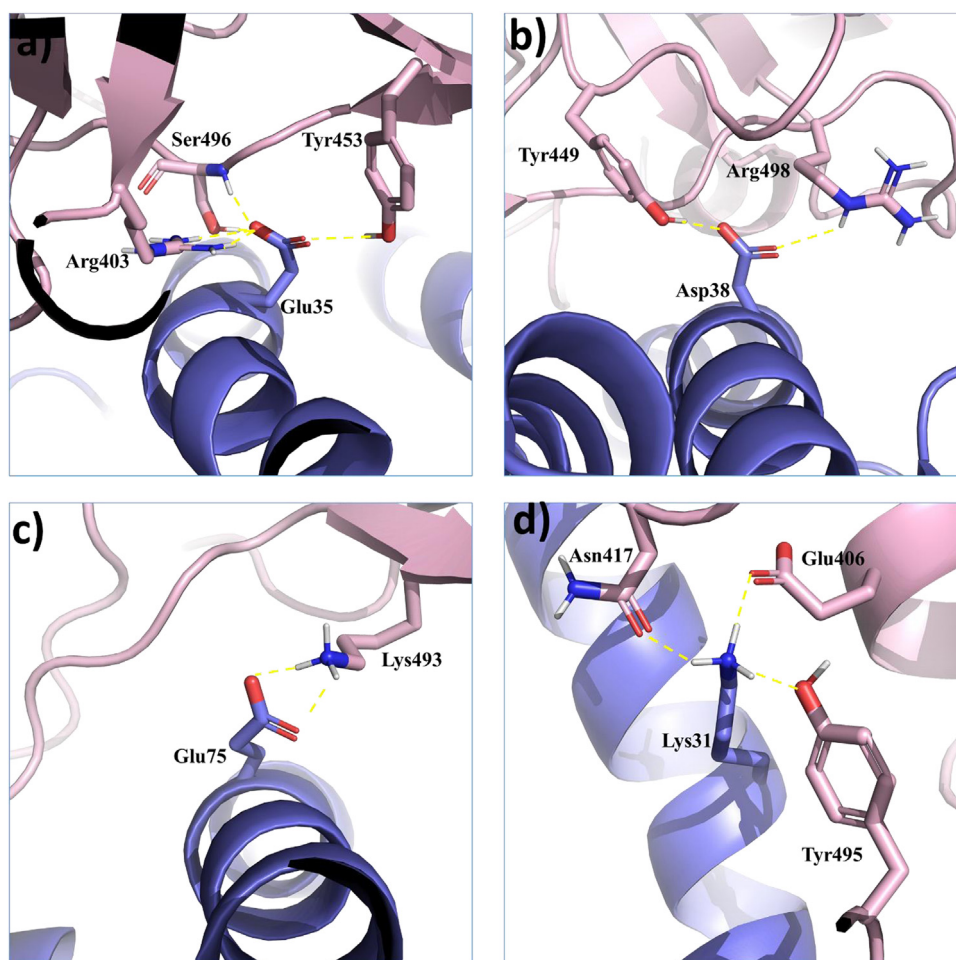


Fig. 7. Key interactions between RBD of Omicron and ACE2

Asp38 of RBD has a further hydrogen bond to Arg498 of ACE2 in Omicron variant in comparison to wild-type Sars-Cov-2 (Tables 1 and 2, Fig. 7(b)). Glu75, which has no interaction in RBD-ACE2 complex of wild-type Sars-Cov-2, make two strong salt-bridges along with two hydrogen bonds in Omicron complex (Tables 1 and 2, Fig. 7(c)). Multiple interactions of key interacting residues in Omicron variant confirm the better binding and higher transmissibility of this variant.

3.4. Role of Spike residue 403 in RBD-ACE2 binding of Omicron variant

Zech et al [36] recently showed that Arg403 play a fundamental role in RBD-ACE2 binding. They reported that a single T403R mutation increases binding of bat sarbecovirus RaTG13 S to hu-

man ACE2 and allows VSV pseudoparticle infection of human lung cells and intestinal organoids. Bat sarbecovirus RaTG13 is a close relative of SARS-CoV-2 which unable to directly infect humans since its Spike (S) protein does not interact efficiently with the human ACE2 receptor. Moreover, previous computational studies suggested that Arg403 is involved in intramolecular interactions and contributes significantly to the strength of SARS-CoV-2 RBD interaction with the human ACE2 receptor [37–40]. Although reactive force field simulations showed that Arg403 can make salt bridge to Glu37 [36], the locations of these two residues are far from each other ($> 6 \text{ \AA}$) in crystal structure [13] (Fig. 8 (a)). Interestingly, our computational results show that Arg403 reach to Glu35 and make two strong salt bridges with it in Omicron variant (Table 1 and Fig. 8 (b)). The new binding interface helps RBD to accommodate Arg403 near Glu35. Based on the pivotal role of Arg403 interaction

Table 3
HADDOCK parameters of the top clusters of Omicron RBD-ACE2 complex

	Cluster 3	Cluster 2	Cluster 4	Cluster 5
HADDOCK score	-187.2 +/- 5.1	-140.0 +/- 5.9	-119.0 +/- 10.1	-106.5 +/- 1.1
Cluster size	33	36	23	11
RMSD from the overall lowest-energy structure	0.3 +/- 0.2	14.1 +/- 0.2	13.4 +/- 0.3	8.7 +/- 0.2
Van der Waals energy	-80.6 +/- 1.8	-66.6 +/- 6.7	-60.7 +/- 5.5	-55.7 +/- 6.2
Electrostatic energy	-524.4 +/- 21.7	-408.5 +/- 38.8	-343.0 +/- 37.9	-236.8 +/- 15.7
Desolvation energy	-15.7 +/- 0.9	-5.7 +/- 2.2	-7.6 +/- 4.5	-16.1 +/- 3.4
Restraints violation energy	139.2 +/- 85.33	140.7 +/- 51.61	178.5 +/- 77.63	126.6 +/- 77.01
Buried Surface Area	2589.4 +/- 71.1	2373.3 +/- 23.3	2242.0 +/- 89.4	1892.5 +/- 79.8
Z-Score	-2.2	-0.8	-0.2	0.2

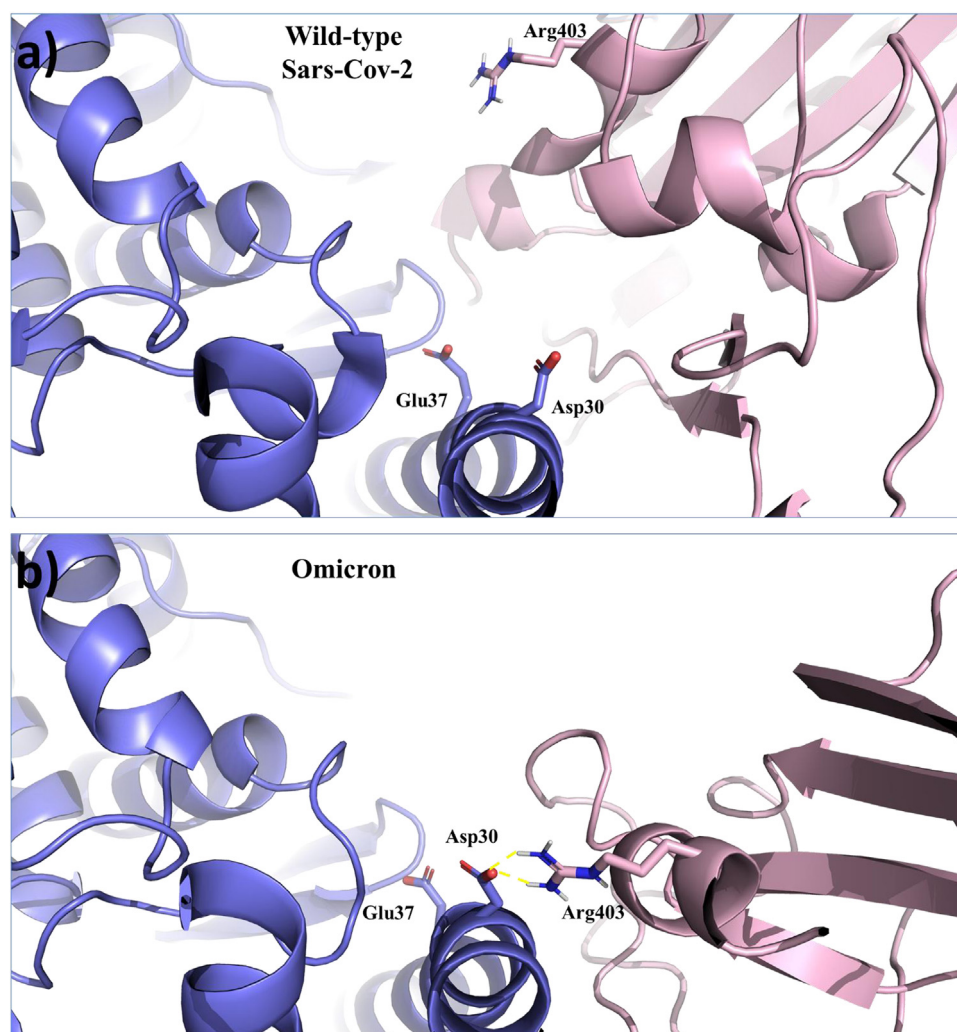


Fig. 8. Locations of Arg403 in wild-type Sars-Cov-2 and Omicron

in Covid-19 infection, it seems that the strong interaction of this residue with Glu35 may also be related to high transmissibility of Omicron variant.

4. Conclusion

WHO recently reported a new VOC of SARS-CoV-2 and named it as “Omicron”. This variant has the most diverse mutations detected during an epidemic, raising serious concerns that it may be associated with a significant reduction in vaccine efficacy and an increased risk of re-infection. It was reported that Omicron is hyper-transmissible in comparison to other Sars-Cov-2 variants. The molecular basis of the high transmission rate of Omicron is not fully understood. RBD domain of SARS-CoV-2 has essential roles in infection and transmission of the virus. It initiates the infection through the interaction with human ACE2. Therefore, studying RBD-ACE2 complex in Omicron can essentially help to understand the molecular mechanism of variant. To obtain a molecular mechanism for high transmission rate of this variant, we have modeled and extensively examined this complex using molecular docking and MD simulations. Interestingly, we found a new binding mode that can be a key in exceptional behavior of Omicron in comparison to other variants. We showed that RBD-ACE2 binding site may drastically relocate with an enlarged interface. This binding site has a larger interface area (about 40%) in comparison to wild SARS-CoV-2. Moreover, this new binding site led to substantial increase (about 80%) in hydrogen bond interactions. We have

evaluated the stability of the predicted complex by MD simulation analysis. The results showed that the complex is significantly stable and does not dissociate after long simulation time. We have extensively examined the interacting residues in wild and Omicron complexes and found that many of these residues are different in two variants. The new binding interface can significantly accommodate R403, as a key RBD residue, near ACE2 surface which leads to two new strong salt bridges. The result of this study can help to understand the molecular basis of fast-spreading properties of Omicron.

Term	Maryam Shirzadeh	Hassan Monhemi	Mohammad Eftekhari
Conceptualization	X	✓	X
Methodology / Study design	X	✓	X
Software	✓	✓	✓
Validation	✓	✓	✓
Formal analysis	✓	✓	✓
Investigation	✓	✓	✓
Resources	✓	✓	✓
Data curation	✓	✓	✓
Writing – original draft	✓	X	X
Writing – review and editing	X	✓	✓
Visualization	X	✓	X
Supervision	X	✓	✓
Project administration	X	✓	X
Funding acquisition	X	✓	X

(✓) indicates contribution and (X) indicates no contribution

Declaration of Competing Interest

The authors declare that they have no known competing financial interests or personal relationships that could have appeared to influence the work reported in this paper.

Data Availability

Data will be made available on request.

Acknowledgments

This work was supported by research council of the University of Neyshabur.

References

- [1] H. Harapan, N. Itoh, A. Yufika, W. Winardi, S. Keam, H. Te, D. Megawati, Z. Hayati, A.L. Wagner, M. Mudatsir, *J. Infect. Public Health* 13 (2020) 667.
- [2] T. Singhal, *Indian J. Pediatr.* 87 (2020) 281.
- [3] WHO.
- [4] B. Hu, H. Guo, P. Zhou, Z.-L. Shi, *Nat. Rev. Microbiol.* 19 (2021) 141.
- [5] W. Ni, X. Yang, D. Yang, J. Bao, R. Li, Y. Xiao, C. Hou, H. Wang, J. Liu, D. Yang, Y. Xu, Z. Cao, Z. Gao, *Critical Care* 24 (2020) 422.
- [6] W.T. Harvey, A.M. Carabelli, B. Jackson, R.K. Gupta, E.C. Thomson, E.M. Harrison, C. Ludden, R. Reeve, A. Rambaut, S.J. Peacock, D.L. Robertson, C.-G.U. Consortium, *Nat. Rev. Microbiol.* 19 (2021) 409.
- [7] I. Martínez-Baz, A. Miqueleiz, I. Casado, A. Navascués, C. Trabajo-Sanmartín, C. Burgui, M. Guevara, C. Ezpeleta, J. Castilla, W.G.f.t.S.o.c.-i. Navarra, *Eurosurveillance* 26 (2021) 2100438.
- [8] Q. Liu, C. Qin, M. Liu, J. Liu, *Infect. Dis. Pover.* 10 (2021) 132.
- [9] K.J. Bruxvoort, L.S. Sy, L. Qian, B.K. Ackerson, Y. Luo, G.S. Lee, Y. Tian, A. Florea, M. Aragonés, J.E. Tubert, H.S. Takhar, J.H. Ku, Y.D. Paila, C.A. Talarico, H.F. Tseng, *BMJ* 375 (2021) e068848.
- [10] D. Vasireddy, R. Vanaparthi, G. Mohan, S.V. Malayala, P. Atluri, *J. Clin. Med. Res.* 13 (2021) 317.
- [11] J. Lopez Bernal, N. Andrews, C. Gower, E. Gallagher, R. Simmons, S. Thelwall, J. Stowe, E. Tessier, N. Groves, G. Dabrera, R. Myers, C.N.J. Campbell, G. Amirthalingam, M. Edmunds, M. Zambon, K.E. Brown, S. Hopkins, M. Chand, M. Ramsay, *N. Engl. J. Med.* 385 (2021) 585.
- [12] GISAID.
- [13] J. Lan, J. Ge, J. Yu, S. Shan, H. Zhou, S. Fan, Q. Zhang, X. Shi, Q. Wang, L. Zhang, X. Wang, *Nature* 581 (2020) 215.
- [14] A. Waterhouse, M. Bertoni, S. Bienert, G. Studer, G. Tauriello, R. Gumienny, F.T. Heer, T.A.P. de Beer, C. Rempfer, L. Bordoli, R. Lepore, T. Schwede, *Nucleic Acids. Res.* 46 (2018) W296.
- [15] C. Dominguez, R. Boelens, A.M.J.J. Bonvin, *J. Am. Chem. Soc.* 125 (2003) 1731.
- [16] G.C.P. van Zundert, J.P.G.L.M. Rodrigues, M. Trellet, C. Schmitz, P.L. Kastiris, E. Karaca, A.S.J. Melquiond, M. van Dijk, S.J. de Vries, A.M.J.J. Bonvin, *J. Mol. Biol.* 428 (2016) 720.
- [17] H.J.C. Berendsen, J.R. Grigera, T.P. Straatsma, *J. Phys. Chem.* 91 (1987) 6269.
- [18] W.F.V. Gunsteren, S.R.B. Billeter, A.A. Eising, P.H. Hunenberger, P. Kruger, A.E. Mark, W.R.P. Scott, I.G. Tironi, (1996).
- [19] H.J.C. Berendsen, J.P.M. Postma, W.F. van Gunsteren, A. DiNola, J.R. Haak, *J. Chem. Phys.* 81 (1984) 3684.
- [20] B. Hess, H. Bekker, H.J.C. Berendsen, J.E.M. Faraaije, *J. Comput. Chem.* 18 (1997) 1463.
- [21] S. Miyamoto, P.A. Kollman, *J. Comput. Chem.* 13 (1992) 952.
- [22] T. Darden, D. York, L. Pedersen, *J. Chem. Phys.* 98 (1993) 10089.
- [23] W.L. Delano, 2002.
- [24] A. Vangone, R. Spinelli, V. Scarano, L. Cavallo, R. Oliva, *Bioinformatics* 27 (2011) 2915.
- [25] J. Shang, G. Ye, K. Shi, Y. Wan, C. Luo, H. Aihara, Q. Geng, A. Auerbach, F. Li, *Nature* 581 (2020) 221.
- [26] J.W. Saville, D. Mannar, X. Zhu, S.S. Srivastava, A.M. Berezuk, J.-P. Demers, S. Zhou, K.S. Tuttle, I. Sekirov, A. Kim, W. Li, D.S. Dimitrov, S. Subramaniam, *bioRxiv* (2021) 2021.09.02.458774.
- [27] L.H.S. Santos, R.S. Ferreira, E.R. Caffarena, W.F. de Azevedo Jr, in: *Docking Screens for Drug Discovery*, Springer New York, New York, NY, 2019, pp. 13–34.
- [28] Z. Jandova, A.V. Vargiu, A.M.J.J. Bonvin, *J. Chem. Theory Comput.* 17 (2021) 5944.
- [29] Z. Feng, M.H. Alqarni, P. Yang, Q. Tong, A. Chowdhury, L. Wang, X.-Q. Xie, *J. Chem. Inf. Model.* 54 (2014) 2483.
- [30] A.C. Pan, D. Jacobson, K. Yatsenko, D. Sritharan, T.M. Weinreich, D.E. Shaw, *Proc. Natl. Acad. Sci.* 116 (2019) 4244.
- [31] L. Martínez, *PLoS One* 10 (2015) e0119264.
- [32] F. Li, W. Li, M. Farzan, S.C. Harrison, *Science* 309 (2005) 1864.
- [33] O. Keskin, B. Ma, R. Nussinov, *J. Mol. Biol.* 345 (2005) 1281.
- [34] I.S. Moreira, P.A. Fernandes, M.J. Ramos, *Proteins Struct. Funct. Bioinf.* 68 (2007) 803.
- [35] I.S. Moreira, P.I. Koukos, R. Melo, J.G. Almeida, A.J. Preto, J. Schaarschmidt, M. Trellet, Z.H. Gümüş, J. Costa, A.M.J.J. Bonvin, *Sci. Rep.* 7 (2017) 8007.
- [36] F. Zech, D. Schniertshauer, C. Jung, A. Herrmann, A. Cordsmeier, Q. Xie, R. Nchioua, C. Prelli Bozzo, M. Volcic, L. Koepke, J.A. Müller, J. Krüger, S. Heller, S. Stenger, M. Hoffmann, S. Pöhlmann, A. Kleger, T. Jacob, K.-K. Conzelmann, A. Ensser, K.M.J. Sparrer, F. Kirchhoff, *Nat. Commun.* 12 (2021) 6855.
- [37] E. Laurini, D. Marson, S. Aulic, M. Fermeglia, S. Prici, *ACS Nano* 14 (2020) 11821.
- [38] E. Laurini, D. Marson, S. Aulic, A. Fermeglia, S. Prici, *ACS Nano* 15 (2021) 6929.
- [39] A.H. Williams, C.-G. Zhan, *J. Phys. Chem. B* 125 (2021) 4330.
- [40] H. Lim, A. Baek, J. Kim, M.S. Kim, J. Liu, K.-Y. Nam, J. Yoon, K.T. No, *Sci. Rep.* 10 (2020) 16862.